A Letters Journal Exploring the Frontiers of Physics

March 2018

EPL, **121** (2018) 68006
doi: 10.1209/0295-5075/121/68006

www.epljournal.org

Effect of solvent viscosity on driven translocation of a semi-flexible chain through a nano-pore

Ramesh Adhikari[a] and Aniket Bhattacharya

Department of Physics, University of Central Florida - Orlando, FL 32816-2385, USA

received 18 October 2017; accepted in final form 27 April 2018
published online 18 May 2018

PACS 87.15.A- – Theory, modeling, and computer simulation
PACS 87.15.H- – Dynamics of biomolecules
PACS 36.20.-r – Macromolecules and polymer molecules

Abstract – We study the effect of the solvent viscosity on the translocation dynamics of a semi-flexible polymer through a nano-pore. We use Langevin dynamics (LD) simulation in two dimensions (2D) and demonstrate that at low viscosity a stiffer chain translocates through a nano-pore faster compared to a more flexible chain and that the order of this translocation time is reversed in the high-viscosity regime. Our simulation data shows a non-monotonic dependence of the mean first passage time (MFPT) on solvent viscosity resulting in a minimum in the MFPT at a particular value of the solvent viscosity. The qualitative behavior of the MFPT of the translocating chain above and below this minimum is different. We have found that the value of the solvent viscosity corresponding to this minimum in MFPT depends on chain stiffness, chain length, applied external bias, and pore radius. We provide physically motivating arguments based on the tension propagation (TP) theory of Sakaue and draw an analogy with the Kramers turnover effect for the non-monotonic dependence of MPFT on viscosity.

Polymer translocation (PT) through a nano-pore (NP) is an important biological transport process. The physics of PT has been studied extensively for more than a decade [1,2] both for the unbiased as well as for the driven translocation. Previous studies have shown that the case of an unbiased or weakly biased translocation through a NP in a solvent with low viscosity can be considered as a *quasi-static* system [3]. When an external bias is present, there have been ample evidences to demonstrate that driven translocation through a NP is a non-equilibrium problem [4–6] which has been adequately captured by the tension propagation (TP) theory of Sakaue [7–9]. In most of the previous studies the external bias and the pore-friction have been used as variables to delineate the signatures of this non-equilibrim process [4–6,10–13].

For the quasi-static case the translocating polymer is viewed as either in equilibrium or close to equilibrium, monomers on each side of the pore wall can be treated as Brownian particles [14]. In this case the relaxation time of the monomers are decoupled from the translocation time. Such process can be solved analytically by mapping the problem into a one-dimensional entropic barrier crossing in terms of the translocation ("s") coordinate [15,16]. The driven PT through a NP on the contrary is a non-equilibrium process [4,5] characterized by the viscous drag on the chain backbone. Such process can be explained by Sakaue's TP theory [7–9]. Ikonen *et al.* [11,12] introduced a Brownian dynamics tension propagation (BDTP) theory by implementing the TP concept into a Brownian dynamics scheme to study the driven translocation of a finite chain characterized by the location of the 1st and the last monomer, and the monomer inside the pore, respectively. In one of our previous publications, we verified this theory numerically for semi-flexible chain by observing the *last-monomer dynamics* [13]. Choosing appropriate parameters for the non-equilibrium system, we found that the MFPT of a semi-flexible chain through a NP is larger than a flexible chain of the same contour length. Later, Luo's group [17,18] also validated our result that for certain conditions, a semi-flexible chain translocates slower than flexible chain. This result is counter-intuitive and follows from the restriction introduced by the NP from a combination of entropy and the viscous drag due to the solvent particles and the NP. On the

[a]Present address: Institute for Computational Engineering and Sciences, University of Texas at Austin - Austin, TX 78712, USA.

contrary de Haan and Slater, on their work [3], showed that a flexible segment of "rod-coil" polymer takes longer than a stiffer segment to translocate through a nano-pore in the *quasi-static* limit. We will show in this paper that this apparent discrepancy arises due to disparate choice of parameters where, among other parameters, solvent viscosity can qualitatively change the results as shown in our recent study that under non-equilibrium condition the more flexible part of a heterogeneous chain translocated faster [19]. In this study we use LD simulation results to further demonstrate that the translocation speed of a flexible and a semi-flexible chain at low and high viscosity can be reversed by changing the solvent condition only, which would then explain and provide a comprehensive understanding of the translocation of stiff and flexible segments through the NP.

Although the solvent viscosity plays an important role in controlling the translocation dynamics, only a few experimental [20,21] and theoretical studies [22–24] have been reported. Previous studies on the effect of solvent viscosity on translocation dynamics showed that the MFPT of a homogeneous flexible chain varies linearly with solvent viscosity in the high-viscosity regime. de Haan and Slater [24] showed that for unbiased translocation, the MFPT is independent of solvent viscosity at low viscosity below a threshold. Luo *et al.* [25] used high and low values of the solvent viscosity to explain slow and fast driven translocation. Some other works [23,24] also present a brief discussion on the influence of solvent viscosity on PT. However, these studies are either for the quasi-static regime or for the non-equilibrium regime of driven translocation.

The purpose of this paper is to show that just by varying the solvent viscosity one can interpolate between the quasi-static and the driven translocation limit and can make qualitative change in the translocation dynamics of stiff and fully flexible chain. i) We show that unlike unbiased translocation, the MFPT for a driven translocation at very low solvent viscosity shows *non-monotonic dependence on viscosity* exhibiting a minimum at a certain value. ii) We will use this result to explain how a flexible/stiff chain translocates faster at high-/low-viscosity regime. iii) We will further show that at high viscosity the translocation thorough a NP is mainly controlled by a viscous drag on the chain backbone, PT at the low viscosity is determined by the combined effect of conformational entropy, pore friction, osmotic pressure from the *trans*-side and an applied external bias.

The non-monotonic dependence of the MFPT on the viscosity motivated us to look at our simulation results in the light of Kramers escape process and turnover effect. As a matter fact the BD formalism that we have used here has been used by others to study the escape rate as a function of the solvent viscosity [26] Admittedly, the original problem has only the solvent friction, while in our case the escape of polymer from the *cis*- to the *trans*-side encounters pore friction and other dynamically changing environment arising out of the conformations of long chain molecule and crowding effect.

The expression for the Kramers escape rate κ is given by [27]

$$\kappa = \Gamma e^{-\Delta h/k_B T}, \tag{1}$$

where Γ is a prefactor which strongly depends on the friction coefficient γ of the system, Δh is the height of the free energy barrier, k_B is Boltzmann constant and T is the absolute temperature. Of particular interest to our study are the results for the escape rates κ_1 and κ_2 in the two extreme limits of very small and large friction, respectively, given by [27–30]:

$$\kappa_1 = \frac{\Delta h e^{-\Delta h/k_B T}}{2\pi k_B T}\gamma, \tag{2a}$$

and

$$\kappa_2 = \frac{\omega_0}{2\pi} e^{-\Delta h/k_B T}\left[\sqrt{1+\frac{\gamma^2}{4\omega_b^2}} - \frac{\gamma}{2\omega_b}\right]. \tag{2b}$$

Here, ω_0 and ω_b are the oscillation frequencies near the bottom of the metastable minimum and near the top of the barrier, respectively. According to these equations, the escape rate increases as friction increases at the low damping limit (eq. (2a)), whereas the rate decreases on increasing the friction at the high damping limit (eq. (2b)). Equations (2a) and (2b) describe the well known "Kramers turnover effect". Evidently, it has been quite tempting to find the rate constant for the whole regime and a large number of authors have addressed this problem and have provided approximate interpolation formulas [30]. One simple method of interpolation between the Kramers two damping limits of the above two equations (eq. (2a) and eq. (2b)) [30] is a linear combination:

$$\kappa^{-1} = a_1\kappa_1^{-1} + a_2\kappa_2^{-1}, \tag{3a}$$

or

$$\langle\tau\rangle = \frac{a_1'}{\gamma} + \frac{1}{\omega_0}\cdot\frac{a_2'}{\left(\sqrt{1+\frac{\gamma^2}{4\omega_b^2}} - \frac{\gamma}{2\omega_b}\right)}. \tag{3b}$$

Here, a_1 and a_2 are two arbitrary dimensionless constants, and the dimensionless quantities a_1' and a_2' are expressed in terms of a_1 and a_2 as follows:

$$a_1' = 2\pi a_1 \cdot \left(\frac{k_B T}{\Delta h}\right) e^{\Delta h/k_B T}, \tag{4a}$$

$$a_2' = 2\pi a_2 \cdot e^{\Delta h/k_B T}. \tag{4b}$$

Despite the complications involved due to contribution of various factors, such as, polymer stiffness, pore friction, crowding on the *trans*-side, etc., surprisingly, we find that this *ad hoc* interpolation scheme captures the "turnover effect" very well (see fig. 1) for the dependence of MFPT

on friction, where we assume that the MFPT is inversely proportional to the escape rate, *i.e.*, $\langle\tau\rangle = \kappa^{-1}$.

We have used a bead spring model [31] of a polymer chain with excluded volume (EV) and performed Langevin dynamics (LD) in 2D using an algorithm proposed by Berendsen and Gunsteren [32] to integrate the Langevin equation. The details of the simulation methods are the same as in our previous publication [13].

Although LD simulation does not include the explicit hydrodynamics, the viscosity of the solvent fluid can be controlled implicitly by the friction coefficient γ. In terms of reduced unit, the viscosity η is equivalent to the friction coefficient ($\eta \sim \gamma$). Using Stoke's relation for solvent at low Reynolds number (in 3 dimensions), one can derive the unit for the viscosity of the implicit solvent to be equivalent to $\tilde{\gamma}/6\pi\sigma$ or $\sqrt{m\epsilon}/6\pi\sigma^2$, where $\tilde{\gamma}$ is the Lennard-Jones (LJ) unit of the monomer friction. Therefore, we observe the effect of solvent viscosity on translocation dynamics via the friction coefficient γ introduced in the Langevin equation.

Similarly in our previous publication [13], the simulation has been carried out in a constant temperature ($T = 1.2\epsilon/k_B$) heat-bath. We used the cut-off for LJ-interaction $r_c = 2^{\frac{1}{6}}\sigma$ and finite extension non-linear elastic (FENE) interaction $R_0 = 1.5\sigma$. The strengths of LJ- and FENE-interactions are fixed at ϵ and $k = 30\epsilon/\sigma^2$, respectively. We vary the chain persistence length ℓ_p by changing the strength of the bending potential κ_b ($\kappa_b = \frac{1}{2}k_BT\ell_p/\sigma$) from 0ϵ to 100ϵ. The simulation results are averaged over at least 2000 independent runs. We present the results of simulation in terms of reduced units.

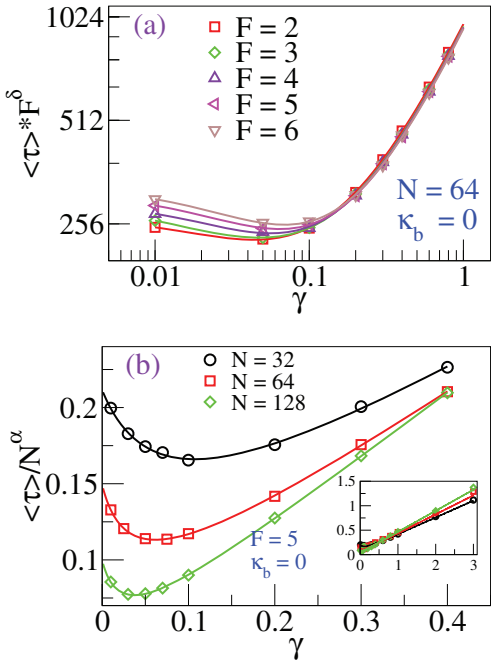

Fig. 1: (Colour online) (a) The log-log plot of MFPT scaled by F^δ ($\delta = 0.9$) as a function of solvent viscosity for various applied external bias (F ranges from 2 to 6) for a fully flexible chain ($\kappa_b = 0$) of length $N = 64$. (b) MFPT scaled by N^α, where $\alpha = 1.5$ is the effective translocation exponent, as a function of solvent viscosity for three different flexible ($\kappa_b = 0$) chains of lengths ($N = 32$, 64, and 128) driven by external bias $F = 5$. The inset shows the effect of γ on scaling $\langle\tau\rangle \sim N^\alpha$ for the wide range of values for γ (0.005 to 3). The solid lines are the simple fit of our simulation data to eq. (3b).

Viscosity dependence of MFPT: The effect of solvent viscosity on a flexible chain translocating through a nano-pore depends on the bias condition. For the unbiased case, the translocation time remains independent of solvent viscosity up to a "threshold viscosity" but increases linearly [24] beyond the threshold. Under the applied external bias, there follows the same trend at high viscosity [22,23]. But at low viscosity, we find that the MFPT changes non-monotonically exhibiting a minimum between two viscosity regimes (high and low). We observe this effect for a flexible chain under various external bias at the pore within the intermediate force regime, *i.e.* for $k_BT/\sigma \leq F \ll (k_BT/\sigma)N^\nu$, where ν is the Flory exponent. Figure 1(a) shows the effect of external bias on the translocation dynamics of a flexible chain over a range (from low to high) of the solvent friction γ. At high solvent viscosity, consistent with previously reported results [10,33], MFPT varies according to $\langle\tau\rangle \sim \gamma/F^\delta$, where δ is an exponent of the order of unity. But, at low-viscosity regime, the applied bias does not follow the same scaling criterion, rather shows a non-monotonic dependence. Our simulation data shows that the MFPT increases as γ decreases in the low-viscosity regime exhibiting a minimum at $\gamma = \gamma_m$. The value of γ_m weakly depends on the applied bias. This weak variation of MFPT with γ in this regime is reflected as a peak (which is larger for stronger bias) in the waiting time distribution near the rear end of the chain. The solid lines in fig. 1(a) and (b) are qualitative fit to eq. (3b) with coefficients a_1' and a_2' which show that our simulation results follow the "Kramers turnover effect". The coefficients carry the combined information of Δh, ω_0 and ω_b. Therefore, the values of these coefficients are different for each of the fitted lines in fig. 1.

Figure 1(b) shows the variation of MFPT for flexible chains of various lengths as a function of solvent friction. Previous studies have established [11,34] that the translocation exponent α ($\langle\tau\rangle \sim N^\alpha$) exhibits a serious finite-size scaling effect. For the range of chain length that we have used for this study ($32 \leq N \leq 128$) the translocation exponent $\alpha \approx 1.5$. We have used this value of α to show scaled plots of MFPT. The inset of fig. 1(b) shows that the effective value of α depends on γ (for the chain lengths considered here, $\alpha < 1.5$ at low viscosity and $\alpha > 1.5$ at high viscosity). In the very narrow range of γ, we find a clear overlap of $\langle\tau\rangle/N^\alpha$ (with $\alpha \sim 1.5$) for three different chain lengths. At high viscosity, we find the variation of $\langle\tau\rangle/N^\alpha$ is completely linear with the slightly different (chain length dependent) slopes as described in previous study for an unbiased translocation [24]. We find the γ_m shifted towards its smaller value for longer chain. This is similar

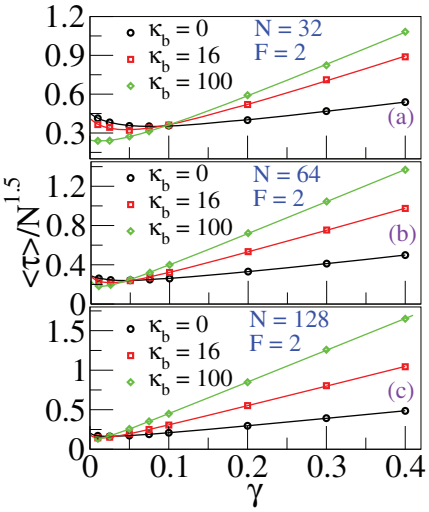

Fig. 2: (Colour online) The effect of viscosity on MFPT of homogeneous chains of different lengths (a) $N = 32$, (b) $N = 64$, and (c) $N = 128$ with different stiffness ($\kappa_b = 0$, 16 and 100). The scaling of $\langle\tau\rangle$ by $N^{1.5}$ helps to compare the strength of influence of viscosity on different chain lengths. The solid lines represent the qualitative fit of our simulation data to eq. (3b).

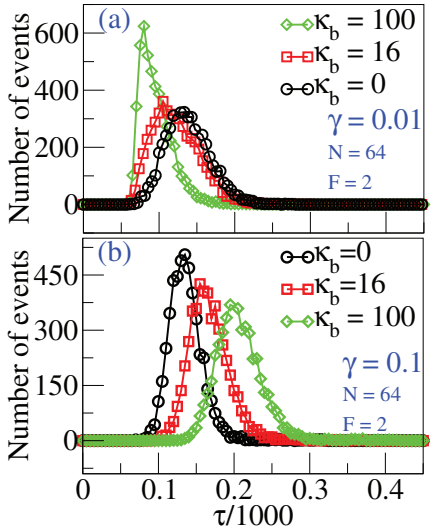

Fig. 3: (Colour online) Histograms of the first passage time for different chain rigidity at (a) $\gamma = 0.01$ and (b) $\gamma = 0.1$ when driven by a small force $F = 2$.

to what reported in ref. [24] where the position of this minimum in the solvent viscosity shifts towards a lower value for a longer chain for the unbiased translocation of a fully flexible chain. This effect, for a longer chain, can be explained as the solvent friction from the bulk in the *cis*-side dominates over the pore friction earlier when the solvent viscosity increases from its smallest value. As mentioned above, at high viscosity, the dynamics of a translocating chain can be described by Sakaue's [7–9] tension propagation (TP) theory. But, at low viscosity, the dynamics is dominated by the pore friction and can be described by "entropic barrier crossing". For unbiased translocation, the system attains its equilibrium state at γ_m (an approximate threshold) below which the MFPT remains almost independent of γ. In this case the chain entropy, the frictional force due to the pore friction and the crowding effect of translocated chain-segments in the *trans*-side control the translocation dynamics [35–39].

The dependence of the solvent viscosity also varies according to the chain stiffness as shown in fig. 2. At high viscosity, we find a stronger dependence of MFPT on γ (larger slope) for a stiffer chain. At low viscosity, we find the non-monotonic variation of MFPT against γ which exhibits the minimum at lower value of γ (*i.e.* $\gamma_m^{flexible} > \gamma_m^{stiff}$). Since the slopes of the τ-γ curve for a flexible chain and a semi-flexible one are different, they cross each other at a certain point which implies that at viscosities lower than the cross-point [3], the stiffer chain translocates faster while above the cross-point the flexible chain translocates faster [19]. In weakly biased condition, the smaller the value of the solvent friction, the closer is the system towards its equilibrium state. The translocation dynamics of a polymer in the equilibrium state can be described as an entropic barrier crossing problem. This regime is narrower for a stiffer chain because of the smaller entropic barrier height. The entropic barrier for a rod-like polymer is negligible, therefore we do not expect the non-monotonic dependence of MFPT on γ. From the simulation data (fig. 2(a) and (b)), we find that there exists, a regime, albeit narrow, where a stiffer chain translocates faster than the corresponding flexible chain of the same length[1].

This non-monotonic dependence is naturally reflected in the histograms of the MFPT which clearly show a crossover when the solvent friction increases from a very low value. In fig. 3, we have plotted the histogram of the first passage time as a function of γ for a driving force $F = 2$ keeping the pore diameter $P_d = 2.0$. It is noteworthy that the order of the peak values for the flexible and stiff chains becomes reversed when γ increases from 0.01 to 0.1. Figure 3 provides conclusive evidence of reversal of MFPT as a function of the solvent viscosity and chain stiffness. As in fig. 1, we have fitted our simulation data in fig. 2 to eq. (3b) with the appropriate fitting coefficients. Although we do not have a deeper understanding of how the polymer translocation through a nano-pore problem can be mapped onto the Kramers barrier crossing problem, the excellent fit for a large number of data sets demonstrates that a simple interpolation scheme of eq. (3b) works well for polymers of different stiffness.

Waiting time distribution: The waiting time distribution shows a clear picture of a translocation process. The time spent by the s-th monomer at the pore is defined as its waiting time $W(s)$, $s = 1, 2, 3, \cdots N$, so that the total

[1] A movie demonstrating this counterintuitive situation can be found online in the supplementary material `suppl1.mpg`, `suppl2.mpg`, `suppl3.mpg` and `suppl4.mpg`.

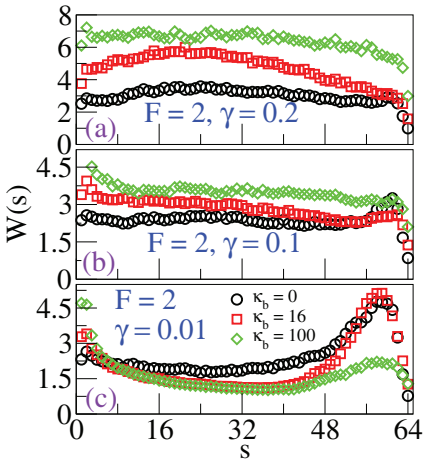

Fig. 4: (Colour online) The waiting time distribution for three different chain rigidity κ_b and for various values (high to low) of solvent viscosities (a) $\gamma = 0.2$, (b) $\gamma = 0.1$ and (c) $\gamma = 0.01$ for chain of length $N = 64$ driven by an weak force $F = 2$.

translocation time of the entire chain is

$$\langle \tau \rangle = \sum_{s=1}^{s=N} W(s). \tag{5}$$

We have shown the data for the waiting time distribution obtained from the simulation of a chain of length $N = 64$ as a function of stiffness at three different values of γ to gain a better understanding of the crossover and reversal of the MFPT (fig. 4(a), (b) and (c)).

At the high-viscosity regime (fig. 4(a)), the non-monotonic curve of the waiting time distribution has two stages representing the *pre-* and *post-* TP processes separated by a peak (see blue curve with symbol "right triangle" in fig. 5(b)) which corresponds to the tension propagation time [11,12]. For a stiffer chain, we observe a flat structure on the waiting time distribution near the position of tension propagation. At low viscosity, we cannot see the peak as in the high-viscosity regime. However, we see a different peak in the waiting time distribution (fig. 4(c)) right before finishing the translocation process for the monomers at the chain end. This peak is due to the combined effect of two resisting forces: pore friction and osmotic pressure from the *trans*-side [35–39], both of which are effective at the low-viscosity regime. The pore friction is determined by its geometry and the velocity of monomers residing inside the pore. The end-monomers of the chain have significantly larger velocity at the pore and hence experience larger pore friction. On increasing the applied bias, the monomer velocity at the pore increases which enhances the resisting force due to pore friction. The frictional force due to the pore friction is [35]

$$f_p \sim \frac{\gamma_p f(t)}{\gamma R(t)}, \tag{6}$$

where $f(t)$ is the total effective force at the pore, $R(t)$ is the length of tensed segment of the chain in the *cis*-side

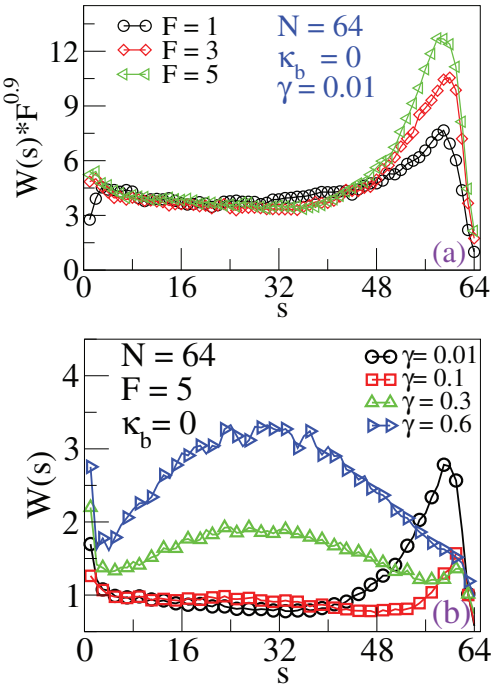

Fig. 5: (Colour online) The waiting time distribution for a flexible chain $\kappa_b = 0$ of length $N = 64$ (a) at low solvent friction $\gamma = 0.01$ for various external biases in the intermediate force range, (b) for various solvent frictions γ when the chain is driven by a constant force $F = 5$.

at time t and γ_p is the effective pore friction. The pore friction can be expressed as $\gamma_p = \frac{A_{pore}}{P_d - 1} + p\gamma$, which has been discussed in ref. [11]. Where, A_{pore} is a constant that depends on the pore geometry and p is the effective number of monomers inside the pore. From the above eq. (6), we know $f_p \propto f(t)$ which is mainly proportional to the external bias F. This implies that the peak on the waiting time distribution, that appeared at the final stage of the translocation process, becomes larger when applied bias is stronger as shown in fig. 5(a). For a stiffer chain the value of $R(t)$ remains larger and since $f_p \propto \frac{1}{R(t)}$, the resisting force at the pore decreases which causes the peak to decrease as the stiffness of the chain increases. The osmotic pressure also resists the translocation process as the number of monomers in the *trans*-side forms crowd in the vicinity of the pore. The force due to this crowding depends on the concentration of monomers in the *trans*-side. For a stiffer chain the concentration of monomers in the *trans*-side becomes smaller. Therefore, the peak in the waiting time distribution becomes smaller and completely disappears for a rod-like chain ($l_p \geq L$). For the unbiased translocation, we do not expect such a peak in the waiting time distribution because the effects of both of the factors are minimized. The height of this peak also decreases (fig. 5(b)) when the solvent viscosity increases. From eq. (6), f_p is significant for very short $R(t)$ (*i.e.* at the end of the chain), for larger $f(t)$ (*i.e* strong applied bias) and at low γ. Since $f_p \propto \frac{\gamma_p}{\gamma}$, we find the peak

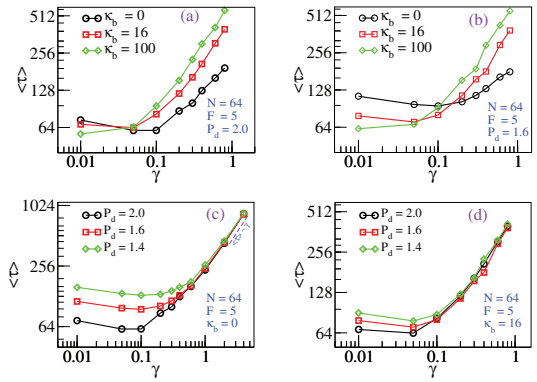

Fig. 6: (Colour online) The MFPT $\langle\tau\rangle$ *vs.* solvent friction as function of chain rigidity $\kappa_b = 0, 16$ and 100 of chain of length $N = 64$ translocating through a nano-pore of diameter (a) $P_d = 2.0$ and (b) $P_d = 1.6$. (c) and (d): the MFPT *vs.* solvent friction for a flexible ($\kappa_b = 0$) and a semi-flexible chain ($\kappa_b = 16$), respectively, when translocating through a nano-pore of different pore-diameters ($P_d = 2.0, 1.6$ and 1.4).

decreases on increasing the value of γ and becomes independent of γ when $\gamma \sim \gamma_p$. For larger value of γ the viscous drag on the chain backbone in the *cis* compartment increases significantly which dominates over the combined effect of pore friction and crowding [36,37].

Effect of pore size: We have studied the effect of solvent friction on PT through NP of different diameters. The minimum of the MFPT curve as a function of solvent viscosity shifts towards a larger value of γ when the pore diameter (P_d) decreases as shown in fig. 6(a) and (b). It is evident that the crossover effect of MFPT for flexible and semi-flexible chain is distinct for narrower pores in the pore-friction–dominated regime. The effect of pore-diameter on translocation decreases gradually when the chain stiffness increases (fig. 6(c), (d)). This is mainly due to the reduced barrier height for a stiffer chain.

In conclusion we have explored the viscosity dependence of MFPT for the driven translocation of a polymer chain using LD simulation in 2D. We compare the translocation speed for a flexible and semi-flexible chain of the same contour lengths from the extreme low- to high-solvent-viscosity regimes. In the high-viscosity regime, the MFPT varies linearly with solvent viscosity for all chains of different flexibility, but the slope of the linearity depends on $\kappa_b \sim \ell_p$. We find a stiffer chain translocates faster in the low-viscosity regime while the order of speed of the translocation is inverted in the high-viscosity regime. In particular, we demonstrate how the probing of chain stiffness using nano-pore sensing depends on solvent viscosity. Furthermore, we find that at very low viscosity, the MFPT varies non-monotonically exhibiting a minimum at a particular value of solvent viscosity γ_m which delineates the qualitatively different behavior of the MFPT below and above this value. We find that γ_m depends on different factors such as: chain length, chain stiffness, pore diameter and applied bias. In the regime of low viscosity, the driven translocation of a more flexible chain is found to be affected more by the frictional force at the pore and osmotic pressure caused by translocated monomers.

Motivated by a large body of investigation to find interpolation schemes from low- to high-viscosity regime, we tried a simple two-parameter scheme. We find that despite additional complexities arising from the chain conformations and pore-polymer interactions, and from the chain stiffness, which in turn controls the crowding, all of our simulation data for different chain length and chain stiffness fit extremely well with the interpolation scheme, suggesting that the Kramers barrier crossing problem has a more universal appeal. A calculation of the barrier height of the translocation problem can in principle provide additional information which lies outside the scope of this paper.

It is also worth mentioning that the lowest value of the parameter γ in this work corresponds to a very small value of viscosity of the real solvent (the viscosity of water at room temperature is $0.001\,\mathrm{kg}\cdot\mathrm{m}^{-1}\mathrm{s}^{-1}$ which is roughly equivalent to $\gamma = 200\,\mathrm{LJ}$ units). However, the real merit of this exercise lies in how solvent viscosity can make the system interpolate from quasi-static to a driven non-equilibrium state. We have also verified that, for the quasi-static system with the choice of a narrower pore and/or shorter chain, the characteristic value of γ (*i.e.*, γ_m) can be shifted towards a higher value comparable to the value of γ used in the several previous LD simulation of PT. Therefore, our findings are relevant and useful for designing NP-based sensors where the translocating chain conformation can be varied from a quasi-static to a non-equilibrium state.

* * *

We are very thankful to Prof. Dr. Ronald Netz for suggesting to analyze our simulation data using Kramers turnover effect. We also thank an anonymous referee for pointing out the additional complexities in the translocation problem not present in the original Kramers barrier crossing problem.

REFERENCES

[1] Muthukumar M., *Polymer Translocation* (CRC Press, Boca Raton) 2011.
[2] Palyulin V. V., Ala-Nissila T. and Metzler R., *Soft Matter*, **10** (2014) 9016.
[3] de Hann H. W. and Slater G. W., *Phys. Rev. Lett.*, **110** (2013) 048101.
[4] Lehtola V. V., Kaski K. and Linna R. P., *Phys. Rev. E*, **82** (2010) 031908.
[5] Bhattacharya A. and Binder K., *Phys. Rev. E*, **81** (2010) 041804.
[6] Bhattacharya A., *Phys. Proc.*, **3** (2010) 1411.
[7] Sakaue T., *Phys. Rev. E*, **76** (2007) 021803.
[8] Saito T. and Sakaue T., *Eur. Phys. J. E*, **34** (2011) 135.

[9] Saito T. and Sakaue T., *Eur. Phys. J. E*, **35** (2012) 125.
[10] Bhattacharya A., Morrison H., Luo K., Ala-Nissila T., Ying S. C., Milchev A. and Binder K., *Eur. Phys. J. E*, **29** (2009) 423.
[11] Ikonen T., Bhattacharya A., Ala-Nissila T. and Sung W., *J. Chem. Phys.*, **137** (2012) 085101.
[12] Ikonen T., Bhattacharya A., Ala-Nissila T. and Sung W., *Phys. Rev. E*, **85** (2012) 051803.
[13] Adhikari R. and Bhattacharya A., *J. Chem. Phys.*, **138** (2013) 204909.
[14] Kantor Y. and Kardar M., *Phys. Rev. E*, **69** (2004) 021806.
[15] Sung W. and Park P. J., *Phys. Rev. Lett.*, **77** (1996) 783.
[16] Muthukumar M., *J. Chem. Phys.*, **111** (1999) 10371.
[17] Zhang K. and Luo K., *J. Chem. Phys.*, **140** (2014) 094902.
[18] Yu W. and Luo K., *Phys. Rev. E*, **90** (2014) 042708.
[19] Adhikari R. and Bhattacharya A., *EPL*, **109** (2015) 38001.
[20] Fologea D., Uplinger J., Thomas B., McNabb D. S. and Li J., *Nano Lett.*, **5** (2005) 1734.
[21] Kawano R., Schibel A. E. P., Cauley C. and White H. S., *Langmuir*, **25** (2009) 1233.
[22] Luan B., Wang D., Zhou R., Harrer S., Peng H. and Stolovitzky G., *Nanotechnology*, **23** (2012) 455102.
[23] Tian P. and Smith G. D., *J. Chem. Phys.*, **119** (2003) 11475.
[24] de Hann H. W. and Slater G. W., *J. Chem. Phys.*, **136** (2012) 154903.
[25] Luo K., Ala-Nissila T., Ying S.-C. and Metzler R., *EPL*, **88** (2009) 68006.
[26] Lonchharich R. J., Brooks B. R. and Pastor R. W., *Biopolymers*, **32** (1992) 523.
[27] Kramers H. A., *Physica*, **7** (1940) 284.
[28] Grabert H., *Phys. Rev. Lett.*, **61** (1988) 1683.
[29] Hänggi P., Talkner P. and Borkovec Michael, *Rev. Mod. Phys.*, **62** (1990) 251.
[30] Linkwitz S., Grabert H., Turlot E., Esteve D. and Devoret M. H., *Phys. Rev. A*, **45** (1992) 3369.
[31] Grest G. S. and Kremer K., *Phys. Rev. A*, **33** (1986) 3628.
[32] van Gunsteren F. and Berendsen H. J. C., *Mol. Phys.*, **45** (1982) 637.
[33] Luo K., Ollila S. T. T., Huopaniemi I., Ala-Nissila T., Pomorski P., Karttunen M., Ying S. C. and Bhattacharya A., *Phys. Rev. E*, **78** (2008) 050901(R).
[34] Ikonen T., Bhattacharya A., Ala-Nissila T. and Sung W., *EPL*, **103** (2013) 38001.
[35] Dubbeldam J. L. A., Rostiashvili V. G. and Vilgis T. A., *J. Chem. Phys.*, **141** (2014).
[36] Saito T. and Sakaue T., *Phys. Rev. E*, **88** (2013) 042606.
[37] Sean D., de Haan H. W. and Slater G. W., *Electrophoresis*, **36** (2015) 682.
[38] Suhonen P. M., Piili J. and Linna R. P., *Phys. Rev. E*, **96** (2017) 062401.
[39] Sarabadani J., Ikonen T., Mokkonen H., Ala-Nissila T., Carson S. and Wanunu M., *Sci. Rep.*, **7** (2017) 7423.